E738 beam production procedure

1 Startup (July 7 morning)

1.1 Beam centering

A 75 MeV/u (2.5427 Tm) $^{12}C^{6+}$ beam is to be delivered to D3. The beam is centered using the profile monitors PR31 (EMS) and PR43 (EMS). As the NMR probes are off center, measured values do not reflect the actual magnetic fields of the central ray. Correction factors have to be determined.

$$B\rho^{\mathrm{PCP}} = \_\_\_\_\_$$

$$c_1 = \frac{B\rho^{\mathrm{PCP}}}{B\rho_1^{\mathrm{NMR}}} = \_\_\_\_\_, \quad c_2 = \frac{B\rho^{\mathrm{PCP}}}{B\rho_2^{\mathrm{NMR}}} = \_\_\_\_\_$$

1.2 Target thickness

The effective thickness of the rotating Be target deviates from the calculation based on the set value of the inclination. Energies of the secondary beam particles are optimized when the target is tilted by 30° (effectively 2309-um thick). The rigidity after the target is 2.3618 Tm (65.042 MeV/u) for $^{12}C^{6+}$.

$$t_{\mathrm{targ}}^{\mathrm{eff}} = \_\_\_\_\_$$

Hereafter, LISE++ simulations are performed assuming an inclination of 30°. Note: in E755, the target thickness was estimated to be 2085 um at "zero degree".

1.3 Wedge thickness

1050-um and 2250-um degraders will be used. 550-um (used for E755) and 750-um thick ones are also attached to the holder. The thicknesses of the wedges will be determined by the $B\rho_2$ values using PR43 (EMS). The target has to be removed beforehand. The primary beam at 2.5427 Tm (75 MeV/u) will be slowed down to 2.4644 Tm (70.609 MeV/u) and 2.3669 Tm (65.313 MeV/u).

$$t_{\mathrm{wedge}}^{1050} = \_\_\_\_\_, \quad t_{\mathrm{wedge}}^{2250} = \_\_\_\_\_$$

1.4 Charge state of ^{12}C

If $^{12}C^{5+}$ is produced at a reasonable rate (100 kpps per 100 nA) needs to be confirmed for the ^{12}C calibration run. The $^{12}C^{20+\rightarrow 20+\rightarrow 19+}$ scheme is adopted to confirm the rate because the PR32 (GAZ) profile monitor cannot be used. The primary beam will be directed onto the wedge without the target. As the charge-state equilibrium thickness is only 1.0 mg/cm^2, the difference of the thicknesses can be neglected.

1.5 Tuning of Caviar, Gallote, and CATS

If the charge state is successfully found, the beam will be sent to D6. We also plan to calibrate the absolute x position of Caviar at the same time.

In E748 a beam of ^{10}Be at $B\rho$ = 1.99 Tm (30 MeV/u) was produced. The deposited energy in between the cathodes (6.4 mm isobutane at 20 mbar) is calculated to be 10 keV. In our case, assuming a magnetic rigidity of 1.7 Tm and the same gas pressure, the energy losses are around 10 keV. We can increase the pressure up to 30 mbar.

^{9}C	60 MeV/u	13 keV
^{8}B	53 MeV/u	10 keV
^{7}Be	44 MeV/u	7.4 keV
^{6}Li	34 MeV/u	5.1 keV

Note: we have tested Caviar using an alpha source. We obtained a timinig efficiency of 97 % under the following condition:

- isobutane 10 mbar
- 700-V bias (tripped at 760 V)
- 4.5-MeV alpha (energy loss in the Kapton window is taken into account)
- energy deposit of 18 keV

If the timing efficiency of Caviar turns out to be unsatisfactory, or the HV trips frequently, we should give up using Caviar. The F31 slits cannot be opened (the limit is about ±1 cm), otherwise the particle identification relying on TCATSHF is impossible whenever ^{6}Li is present in the cocktail beam.

Gallote will also be used as an auxiliary detector. Tuning?

2 ^{10}C setting (July 7 afternoon)

2.1 PID without wedge

The 1050-um wedge will be used for the radioactive beams. $B\rho_1$ = 1.9362 Tm, $B\rho_2$ = 1.9362 Tm (62.814 MeV/u). F31 ±0.6 mm, F43 ±30 mm. ^{10}C at 4400 pps per 100 nA is expected. The RF period is assumed to be 76 ns for producing TE2D4HF plots.

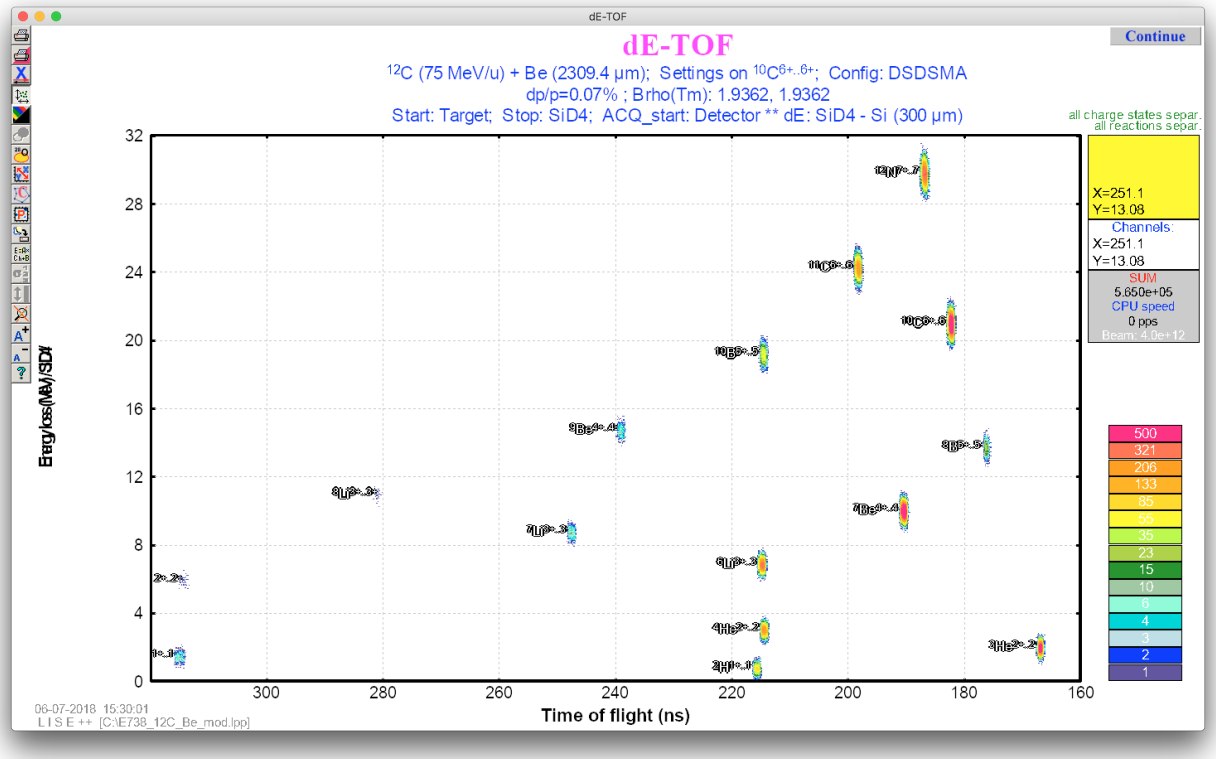

Figure 1: ^{10}C setting, without wedge, F31 ±0.6 mm, F43 ±30 mm, E2D4-TE2D4 absolute TOF.

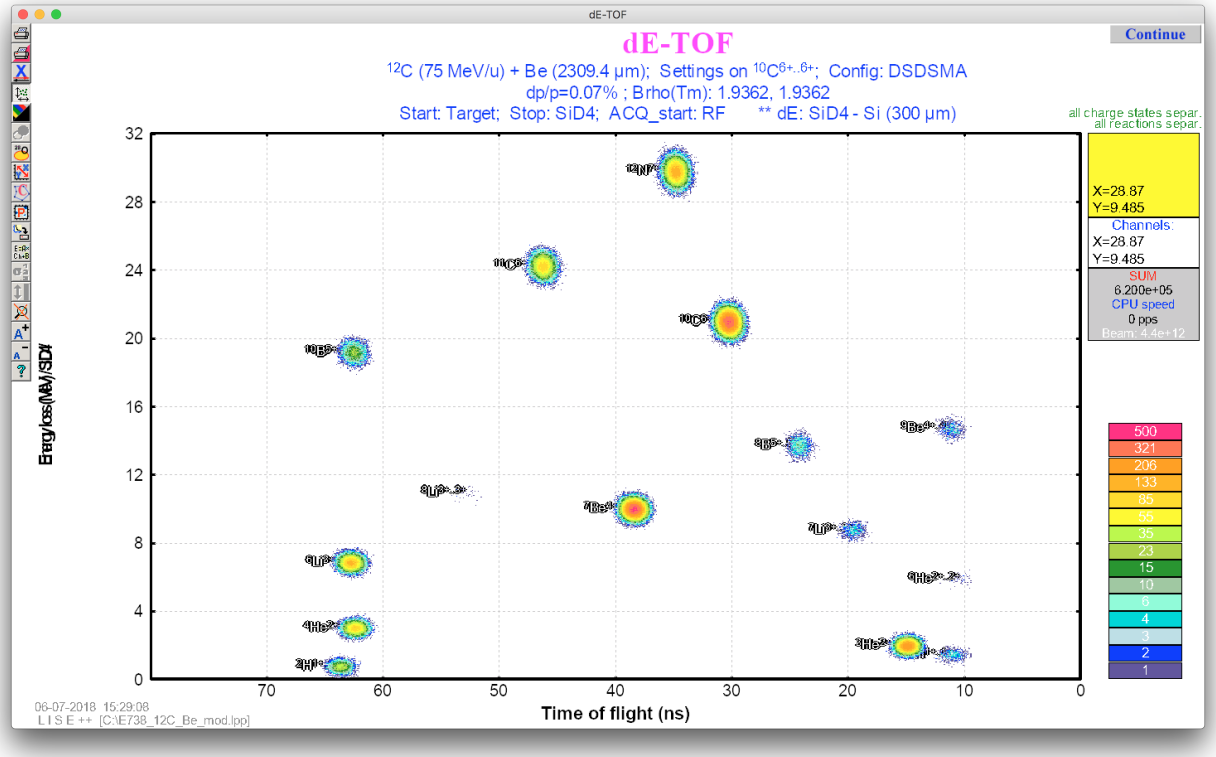

Figure 2: ^{10}C setting, without wedge, F31 ±0.6 mm, F43 ±30 mm, E2D4-TE2D4HF.

We set $B\rho_1 = B\rho_2 = 1.8362$ Tm (56.674 MeV/u) so that the energy losses reamain the same. The counting rate of ^{10}C should decrease (1000 pps per 100 nA), while the yield of ^{8}B is expected to increase.

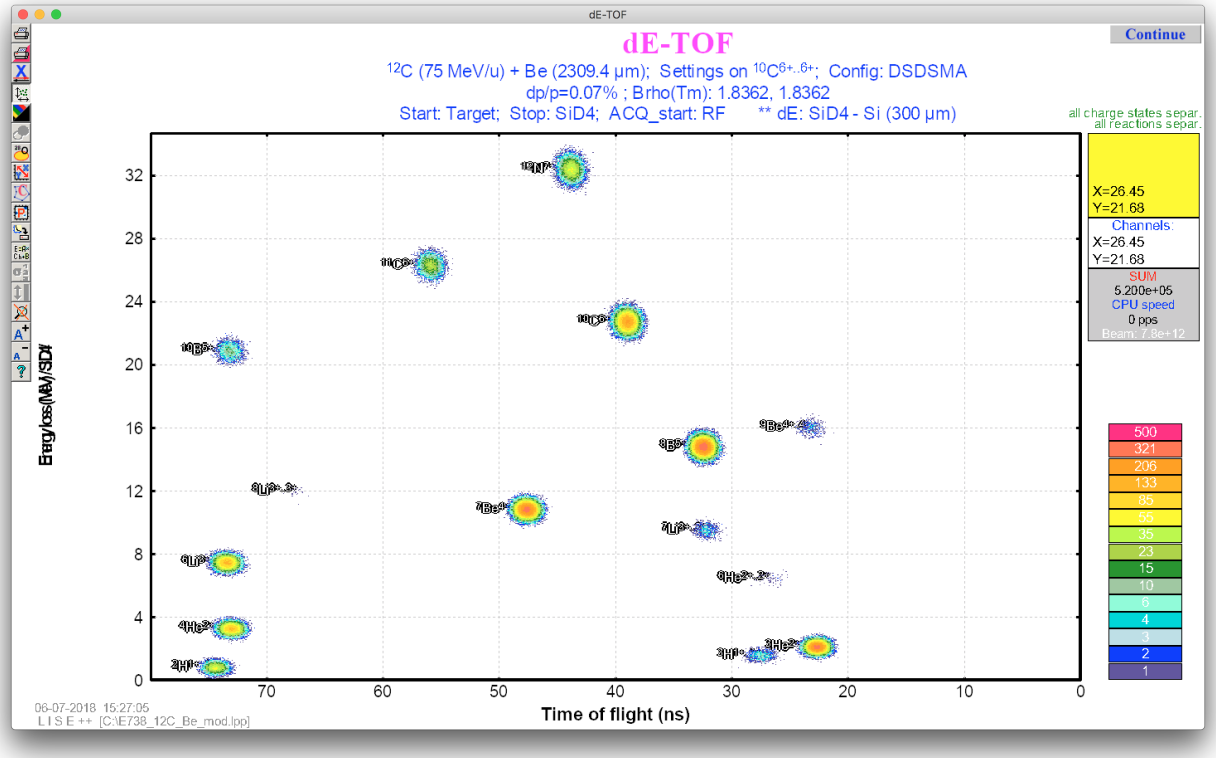

Figure 3: ^{10}C setting, $B\rho_1 = B\rho_2$, F31 ±0.6 mm, F43 ±30 mm, E2D4-TE2D4HF.

2.2 PID with wedge

$B\rho_1$ = 1.9362 Tm, $B\rho_2$ = 1.8362 Tm (56.674 MeV/u). F31 ±0.6 mm, F43 ±30 mm. ^{10}C at 3500 pps per 100 nA is expected. Counting rates of others are much less (two orders of magnitude at least).

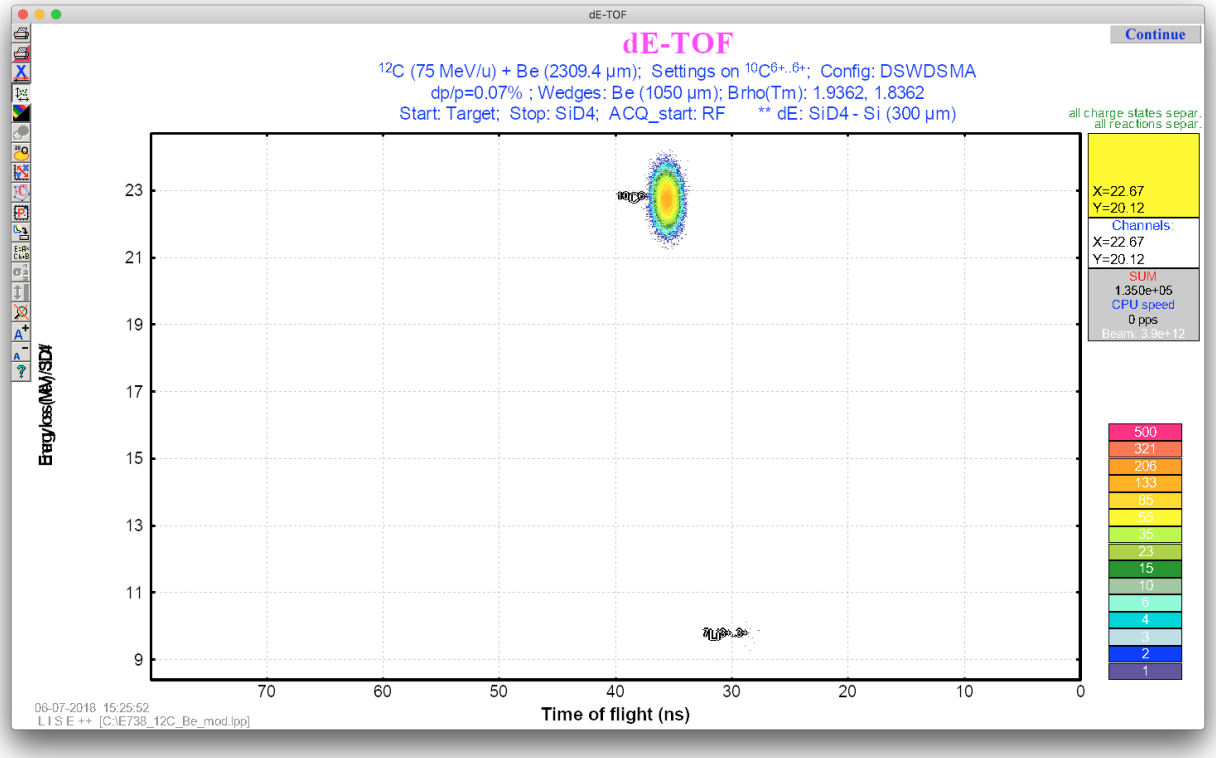

Figure 4: ^{10}C setting, with wedge, F31 ±0.6 mm, F43 ±30 mm, E2D4-TE2D4HF.

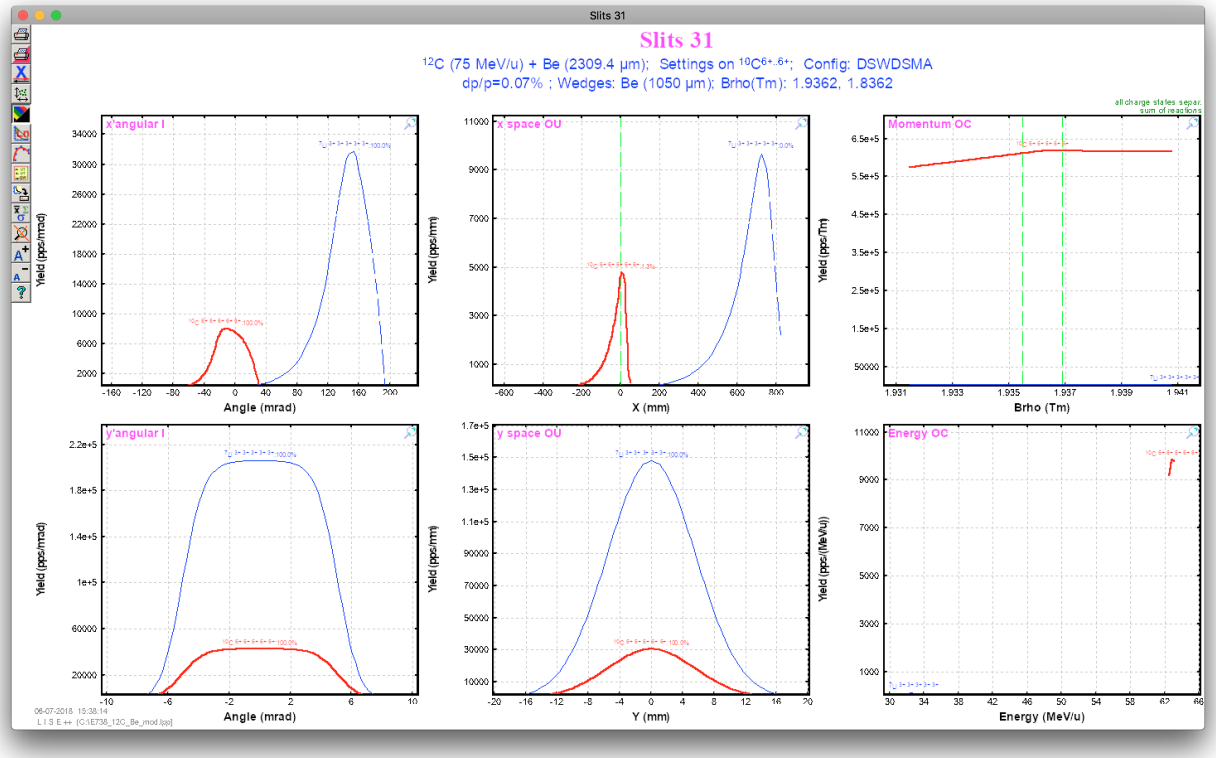

Figure 5: ^{10}C setting, with wedge, F31 ±0.6 mm, F43 ±30 mm, F31 distributions.

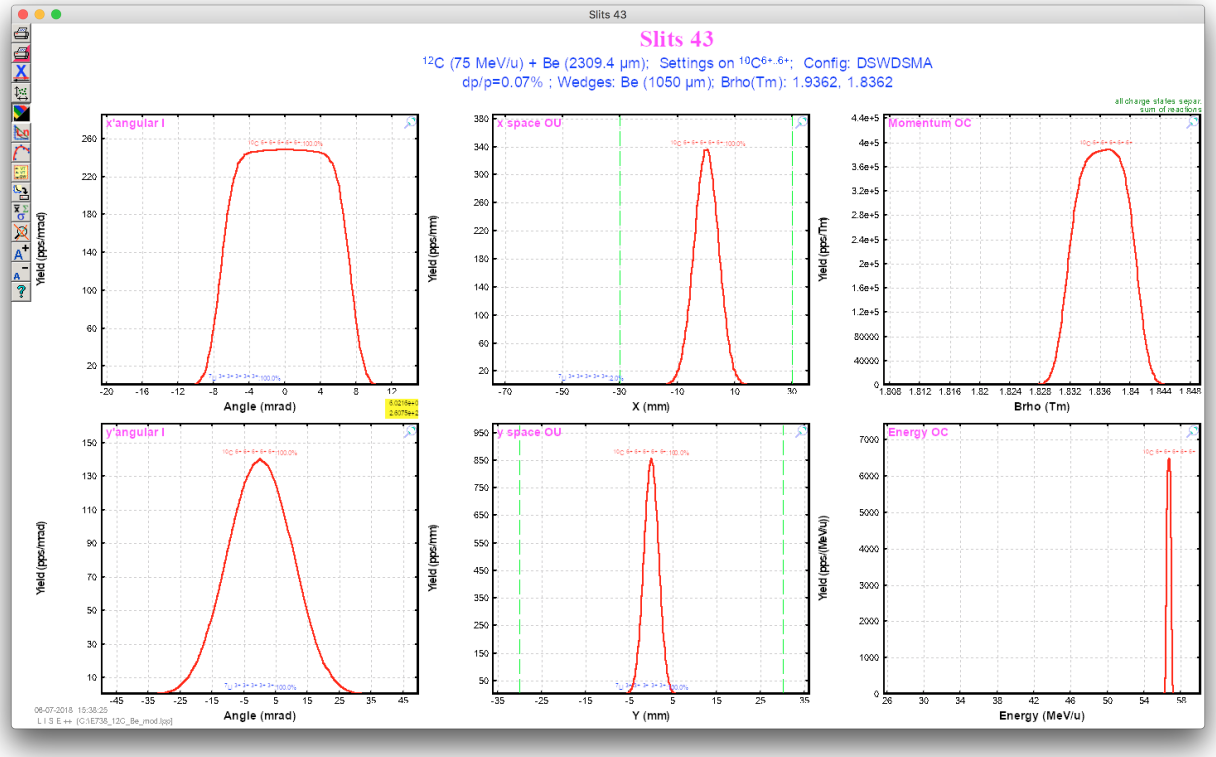

Figure 6: ^{10}C setting, with wedge, F31 ±0.6 mm, F43 ±30 mm, F43 distributions.

2.3 D6

F43 will be closed to improve the purity. The expected rate at D6 is 3500 pps per 100 nA when F31 is sligtly opened (±1.0 mm).

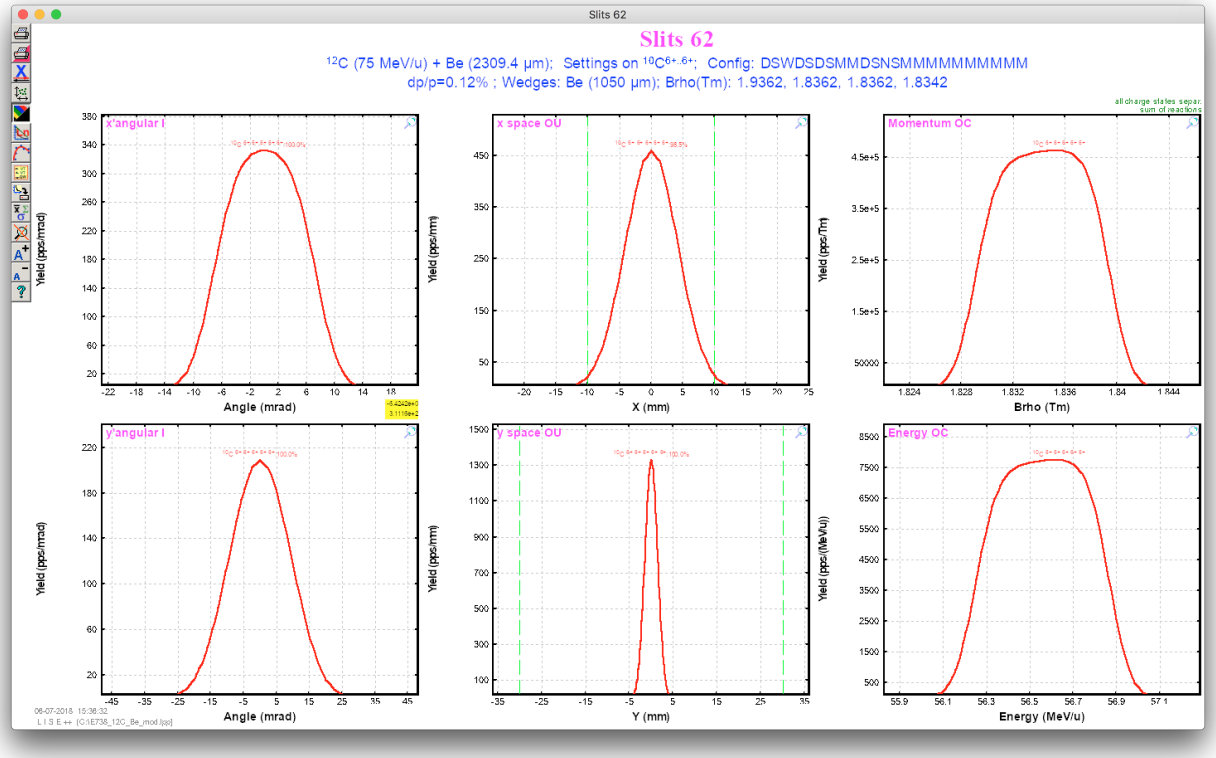

Figure 7: ^{10}C setting, F31 ±1.0 mm, F43 ±10 mm, F62 distributions.

3 ^{9}C setting (July 9 morning)

3.1 PID without wedge

$B\rho_1$ = 1.7279 Tm, $B\rho_2$ = 1.7279 Tm (61.587 MeV/u for ^{9}C). F31 ±0.6 mm, F43 ±30 mm. Expected yields are shown below. The values are scaled with respect to 100 nA.

^{9}C	1.9×10^2 pps
^{8}B	5.5×10^2 pps
^{7}Be	5.1×10^2 pps
^{6}Li	2.6×10^2 pps

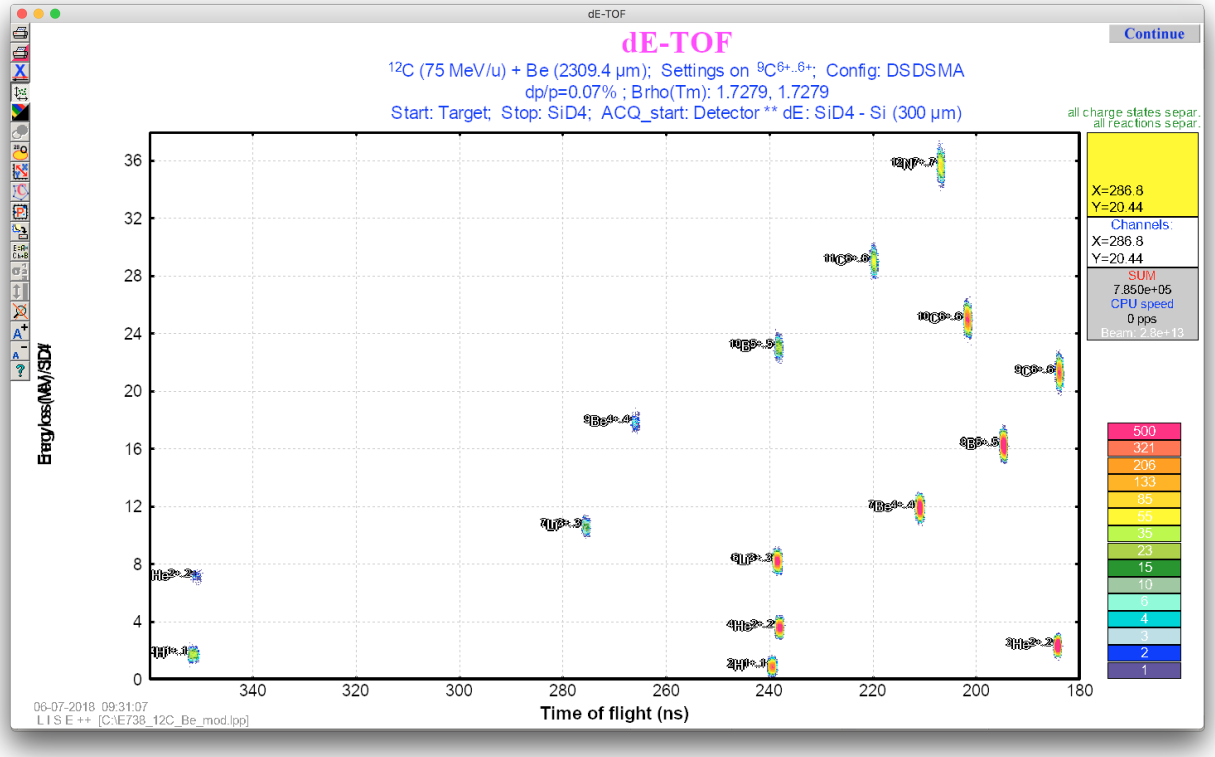

Figure 8: ^{9}C setting, without wedge, F31 ±0.6 mm, F43 ±30 mm, E2D4-TE2D4 absolute TOF.

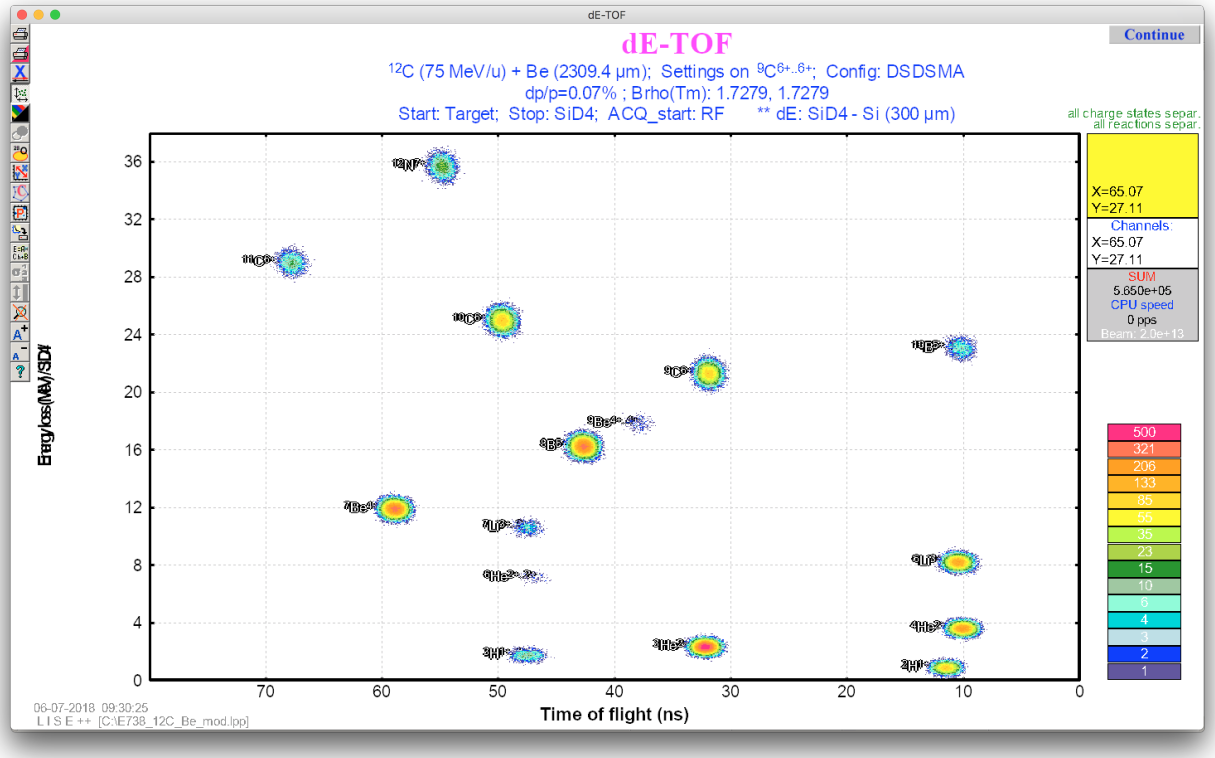

Figure 9: ^{9}C setting, without wedge, F31 ±0.6 mm, F43 ±30 mm, E2D4-TE2D4HF.

We set $B\rho_1 = B\rho_2 = 1.6243$ Tm (54.621 MeV/u) so that the energy losses remain the same.

^{9}C	6.7×10^{1} pps
^{8}B	1.8×10^{2} pps
^{7}Be	1.9×10^{2} pps
^{6}Li	1.3×10^{2} pps

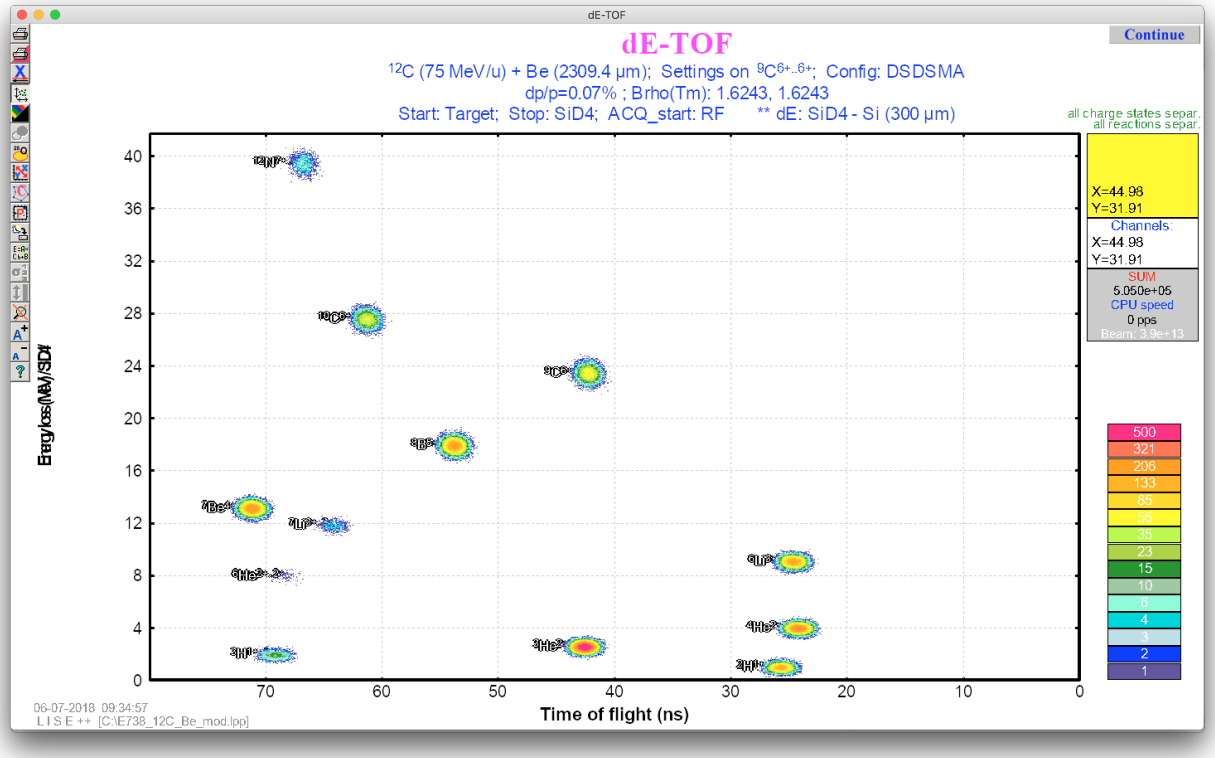

Figure 10: ^{9}C setting, $B\rho_1 = B\rho_2$, F31 ±0.6 mm, F43 ±30 mm, E2D4-TE2D4HF.

3.2 PID with wedge

$B\rho_1 = 1.7279$ Tm, $B\rho_2 = 1.6243$ Tm (54.621 MeV/u for ^{9}C). F31 ±0.6 mm, F43 ±30 mm. Expected rates and energies at F43 are shown below.

^{9}C	1.5×10^{2} pps	54.6 MeV/u
^{8}B	4.1×10^{2} pps	48.4 MeV/u
^{7}Be	3.7×10^{2} pps	40.7 MeV/u
^{6}Li	1.8×10^{2} pps	31.1 MeV/u

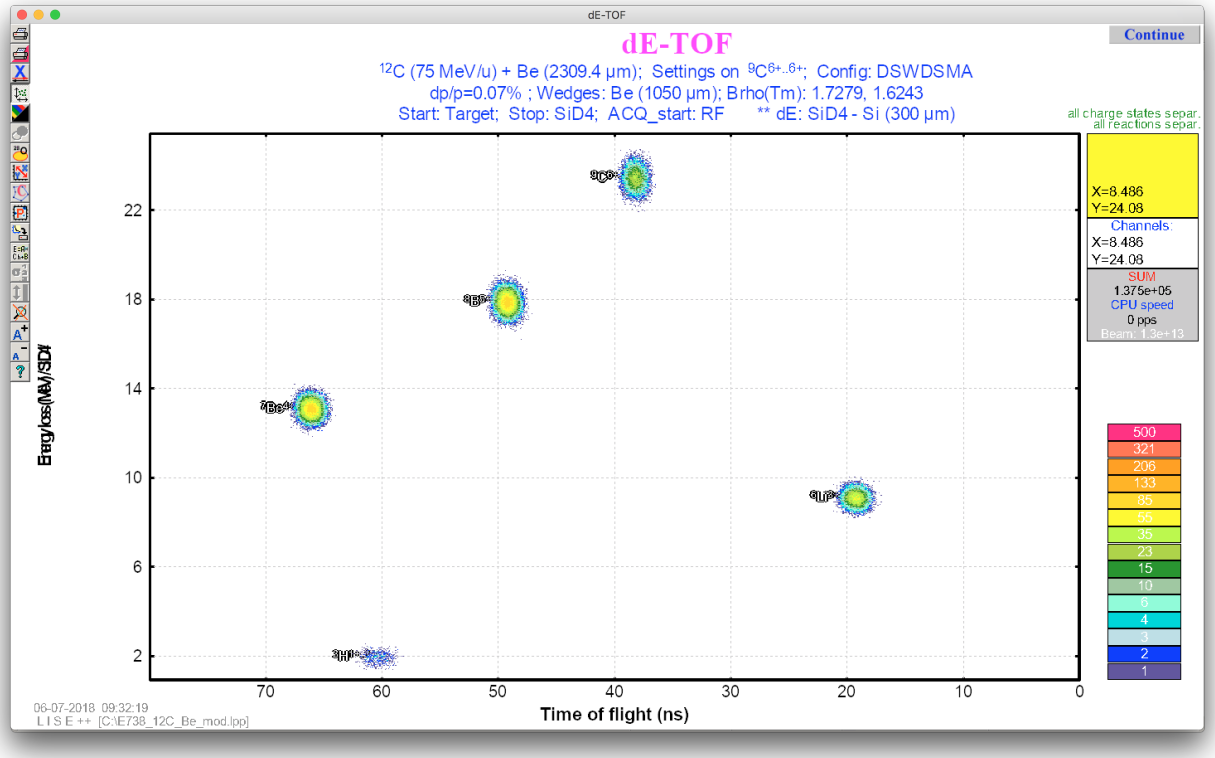

Figure 11: ^{9}C setting, with wedge, F31 ±0.6 mm, F43 ±30 mm, E2D4-TE2D4HF.

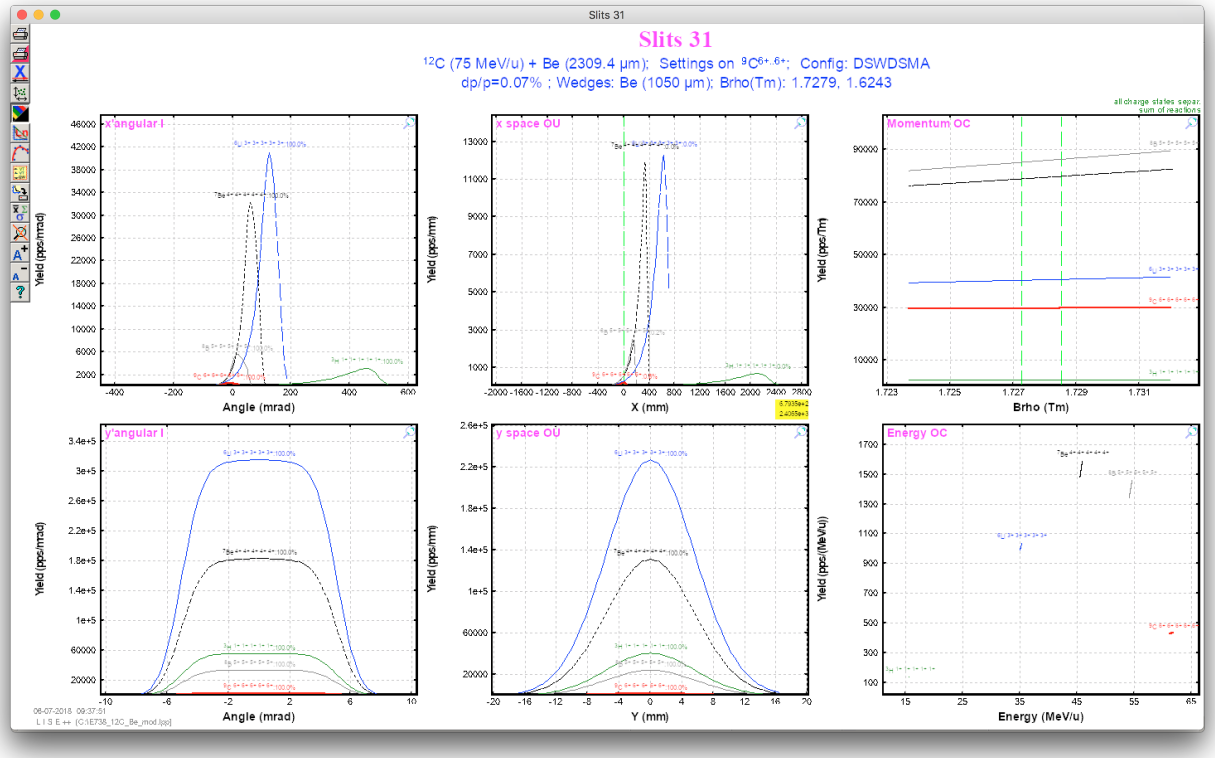

Figure 12: ^{9}C setting, with wedge, F31 ±0.6 mm, F43 ±30 mm, F31 distributions.

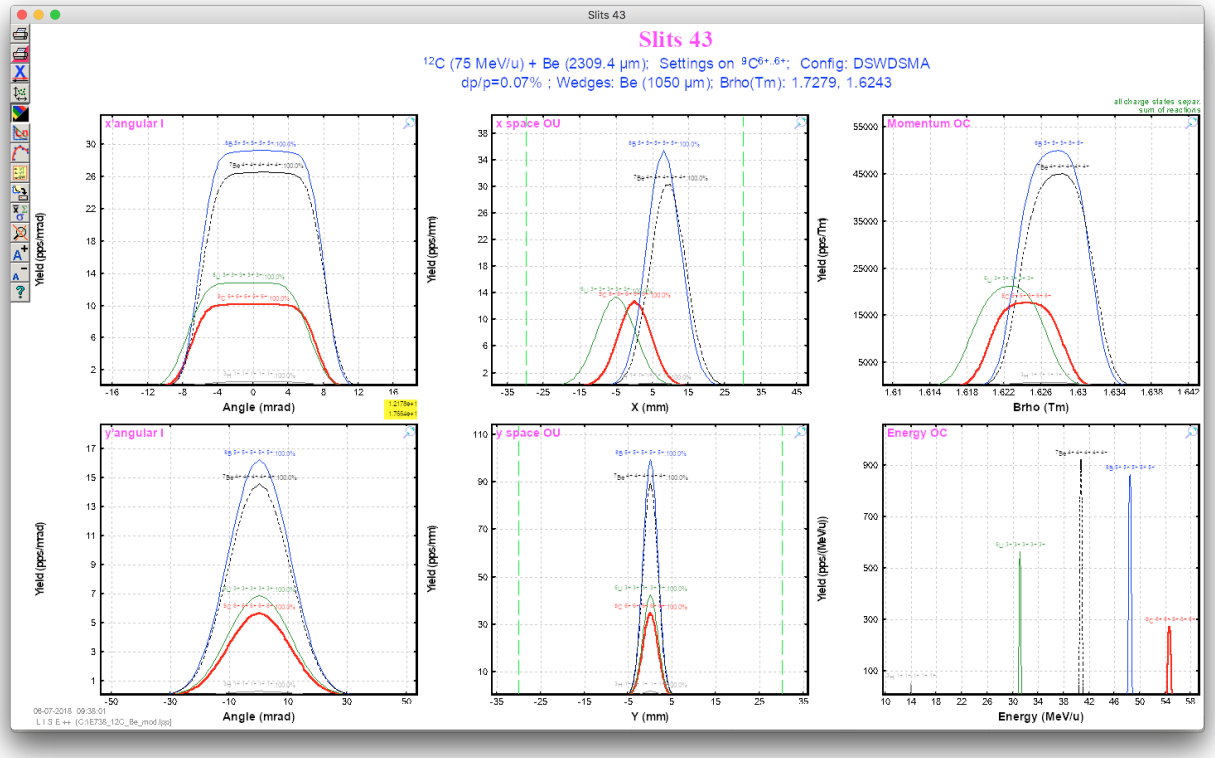

Figure 13: ^{9}C setting, with wedge, F31 ±0.6 mm, F43 ±30 mm, F43 distributions.

3.3 D6

The beam will be sent to D6. The TCATSHF (and also TE2D6) timings of ^{6}Li and ^{7}Be are overlapping.

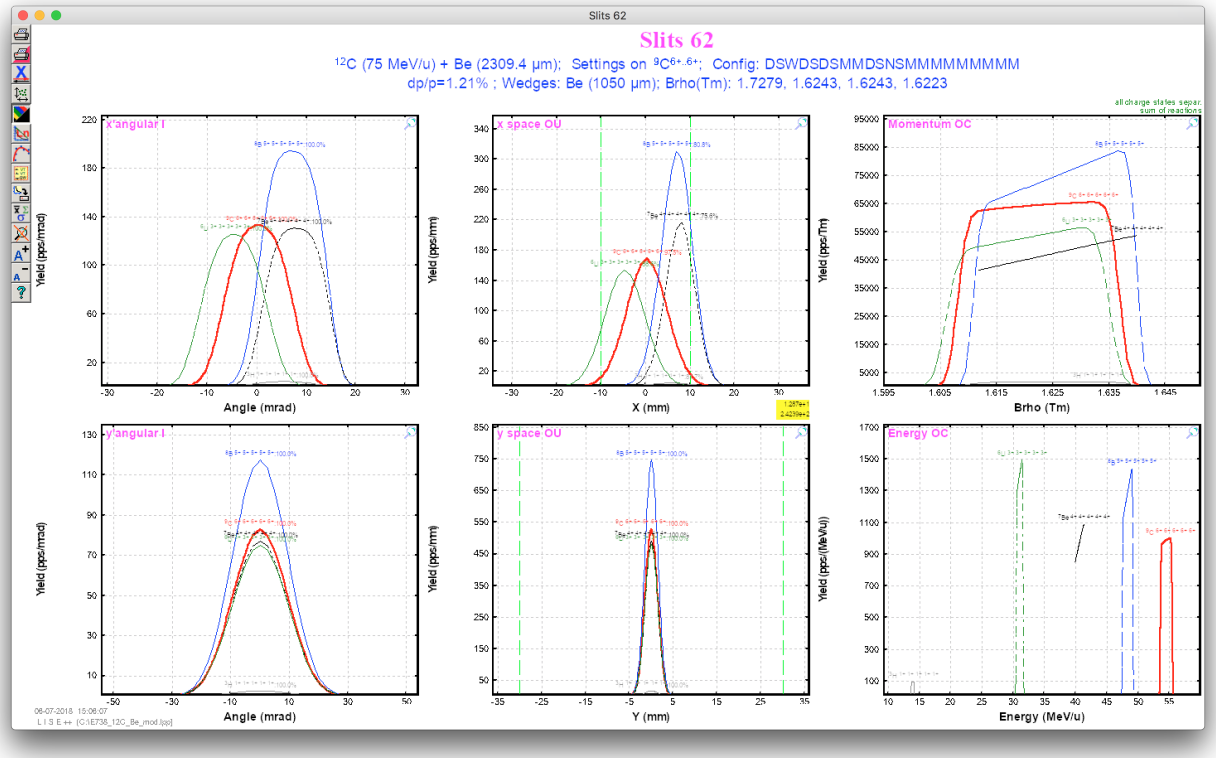

Figure 14: ^{9}C setting, F31 ±10 mm, F43 ±10 mm, F62 distributions.

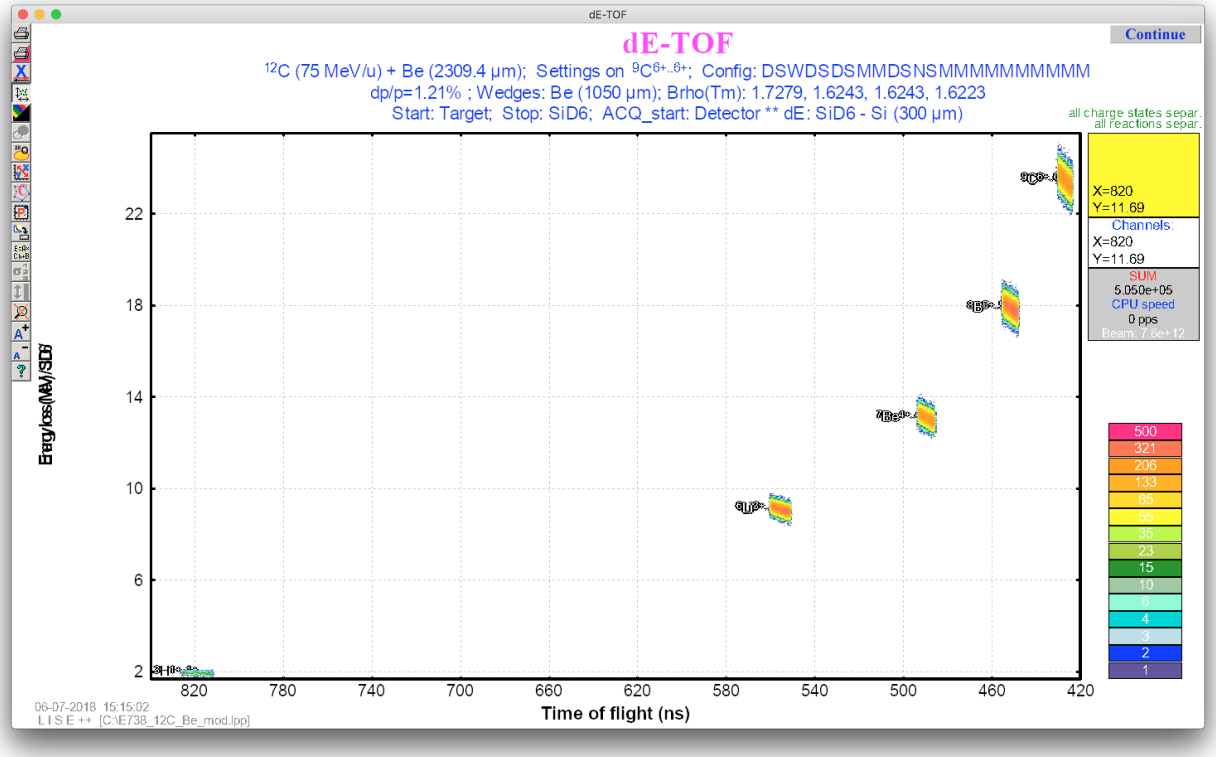

Figure 15: ^{9}C setting, F31 ±10 mm, F43 ±10 mm, E2D6-TE2D6HF absolute TOF.

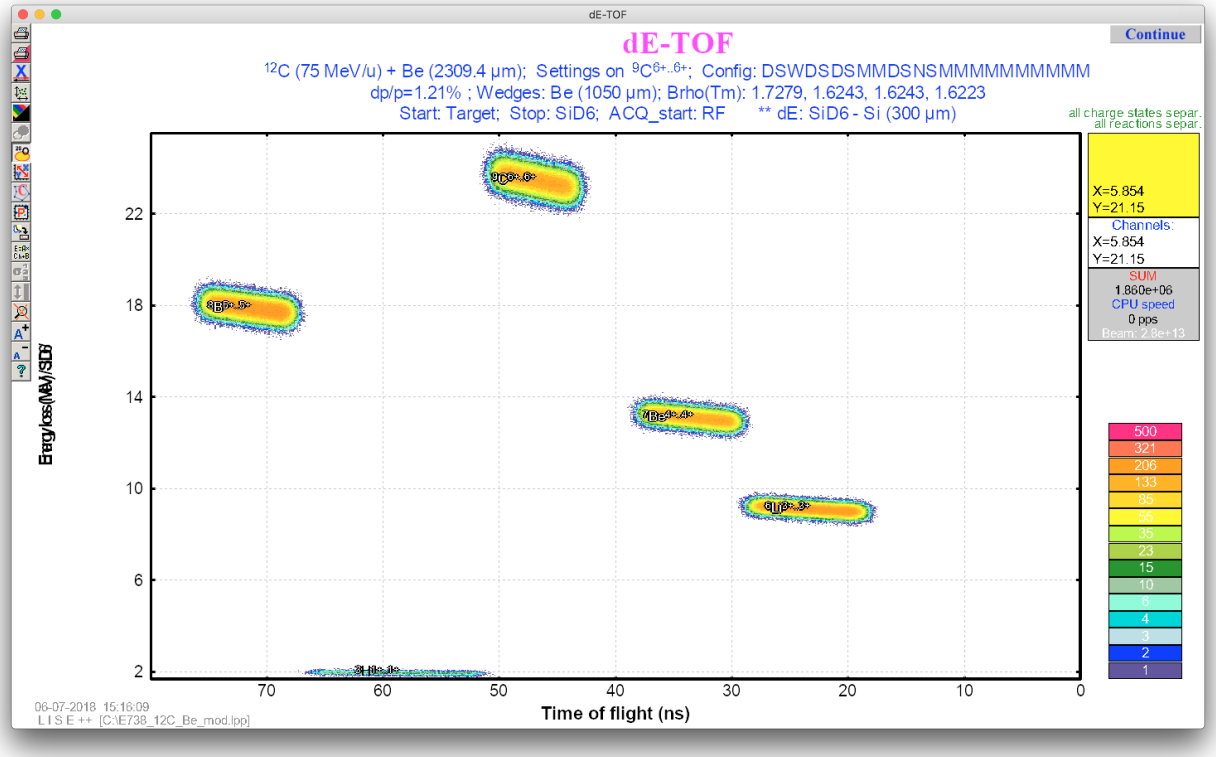

Figure 16: ^{9}C setting, F31 ±10 mm, F43 ±10 mm, E2D6-TE2D6HF.

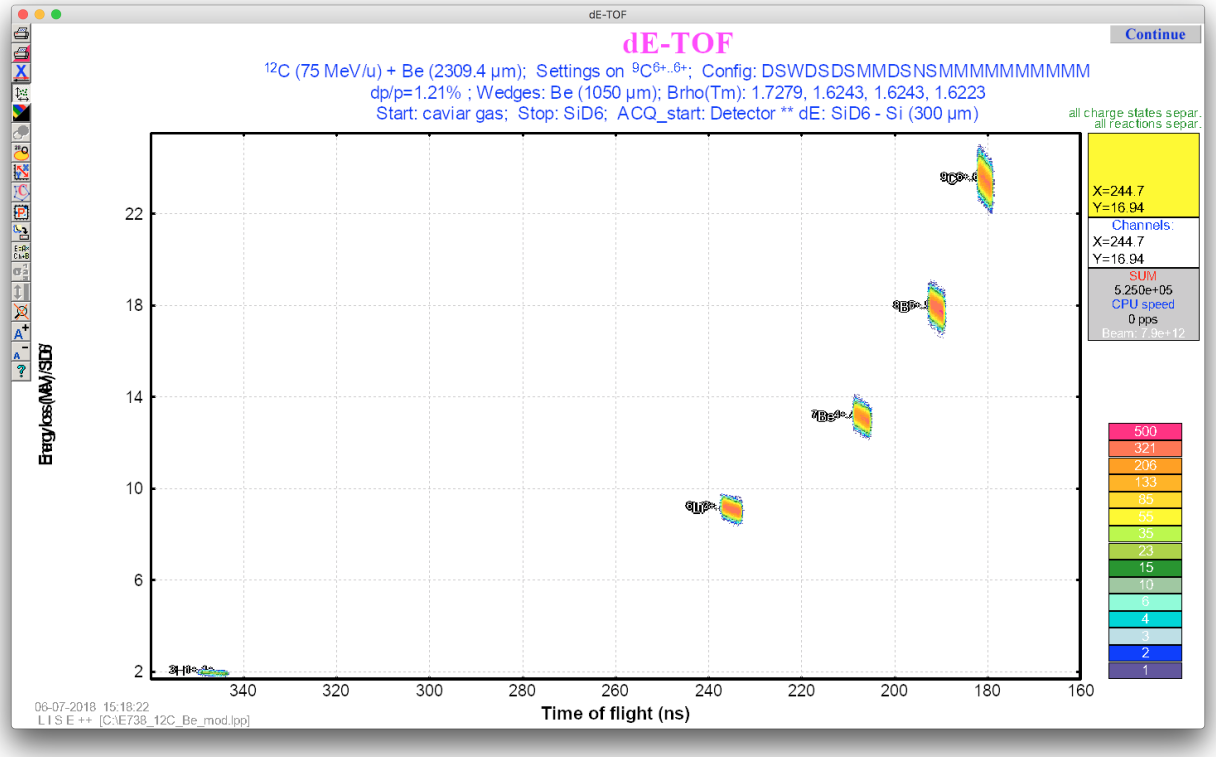

Figure 17: ^{9}C setting, F31 ±10 mm, F43 ±10 mm, E2D6-TCATSCAV.

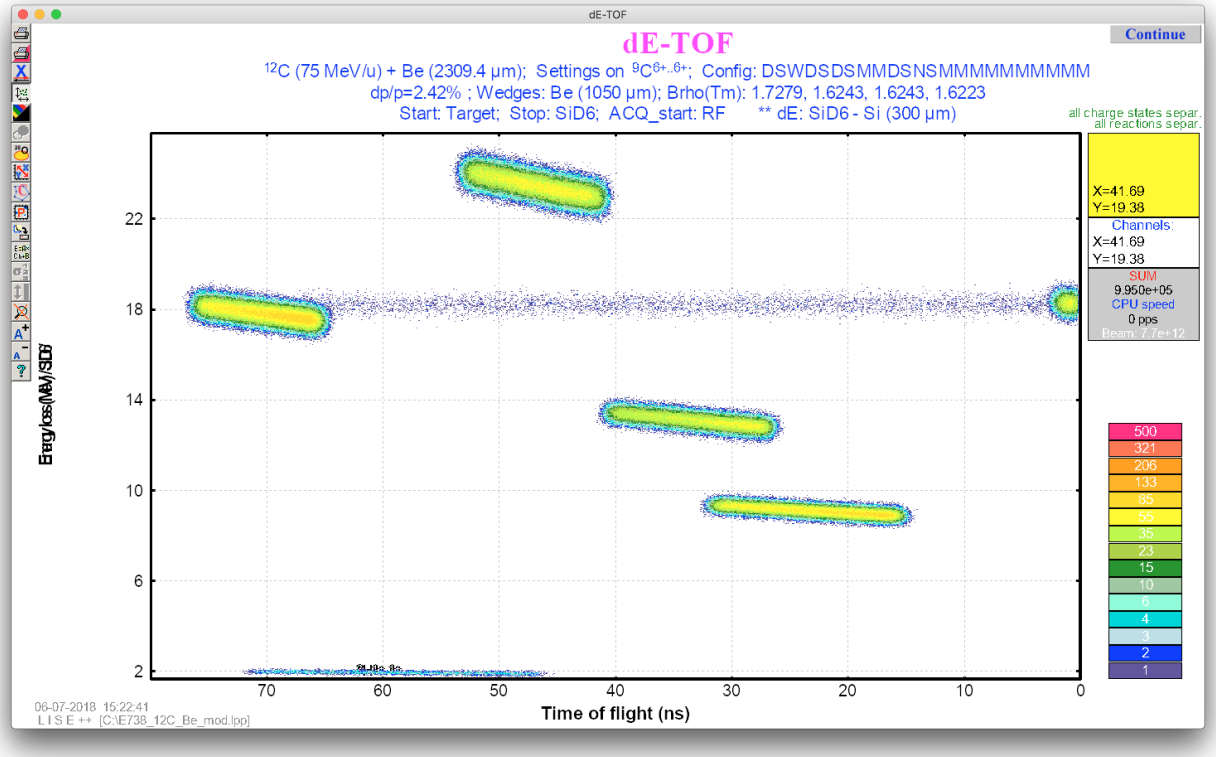

Figure 18: ^{9}C setting, F31 ±20 mm, F43 ±10 mm, E2D6-TCATSCAV.

Predictions of beam intensities assuming a 100 nA intensity. The values scale almost linerly with F31.

F31	±10 mm	±20 mm	±30 mm
$\Delta p/p$	1.2 %	2.4 %	3.6 %
^{9}C	1.9×10^3	3.6×10^3	5.0×10^3
^{8}B	2.2×10^3	4.3×10^3	6.5×10^3
^{7}Be	1.3×10^3	2.4×10^3	3.4×10^3
^{6}Li	1.5×10^3	3.1×10^3	4.5×10^3

3.4 Wien filter

The Wien filter need to be activated if the rate of ^{6}Li is high. 3000 kV/m is assumed.

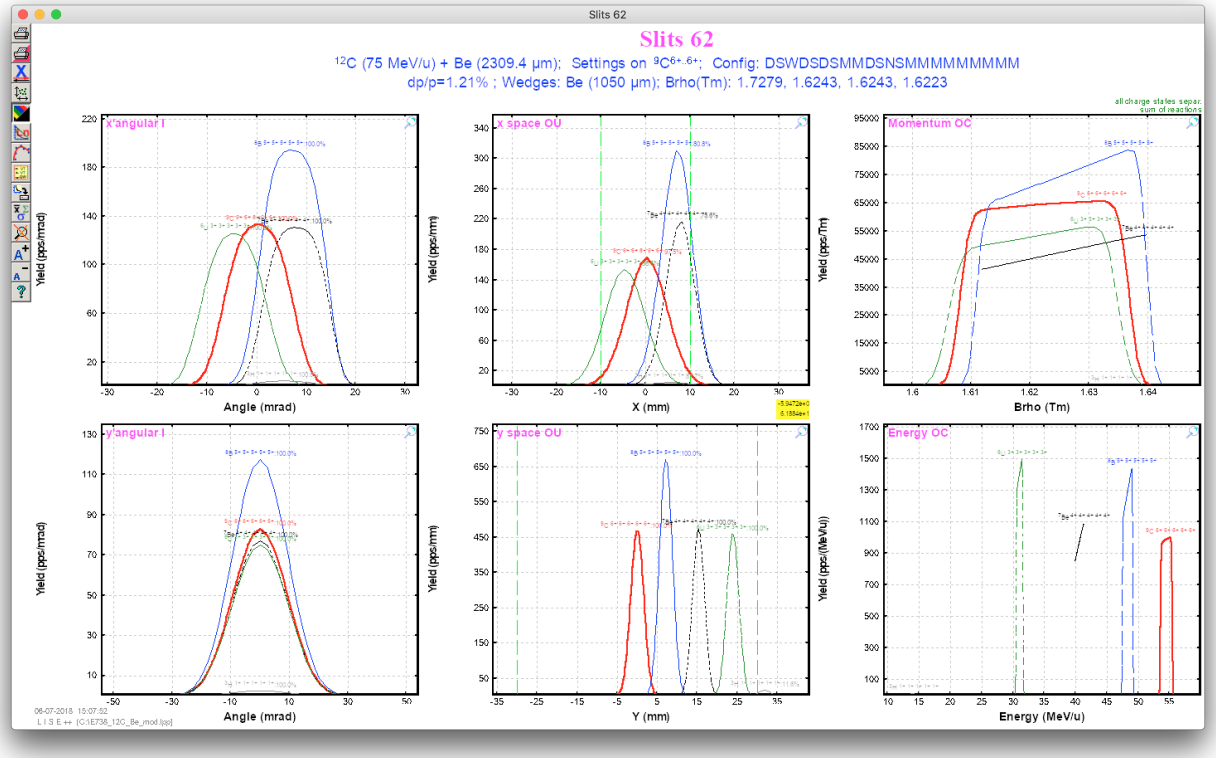

Figure 19: ^{9}C setting, F31 ±10 mm, F43 ±10 mm, WF at 3000 kV/m.

4 ^{12}C setting (July 14 morning)

4.1 Charge state

The wedge thickness will be changed from 1050 um to 2250 um to lower the energy. The $^{12}C^{20+\rightarrow 19+\rightarrow 20+}$ scheme will be adopted as in E755. The beam is slowed down to 2.1465 Tm (54.033 MeV/u $^{12}C^{6+}$). Cf. Charge calculations for Ca and Be, simulating E755 and E748. The main concern is that the fraction of the Hydrogen-like is too small for C ions (see the Charge calculation, the order of 1×10^{-6}). However, the use of $^{12}C^{5+}$ is still feasible with a 100 nA primary beam, corresponding to 1×10^{11} pps. If it fails, we may ask a faint beam at 0.1 pA to get 1.0×10^5 pps, which is unlikely to be stable.

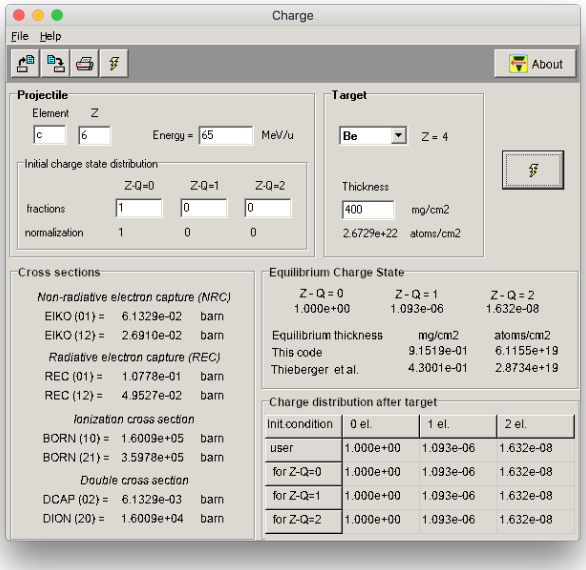

Figure 20: Charge state distribution of C ions at 65 MeV/u.

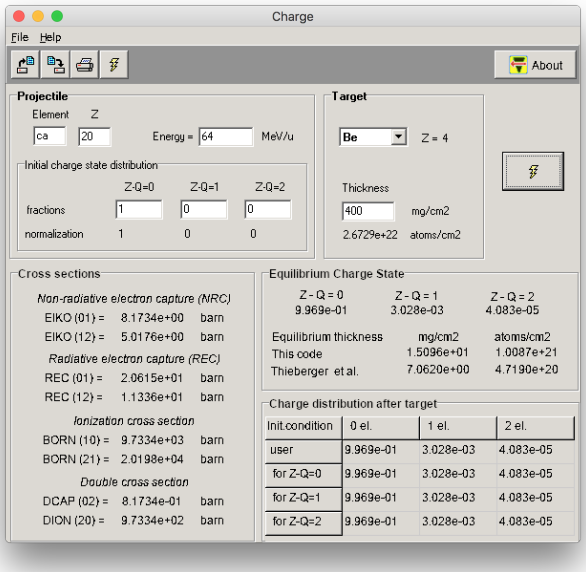

Figure 21: Charge state distribution of Ca ions at 64 MeV/u.

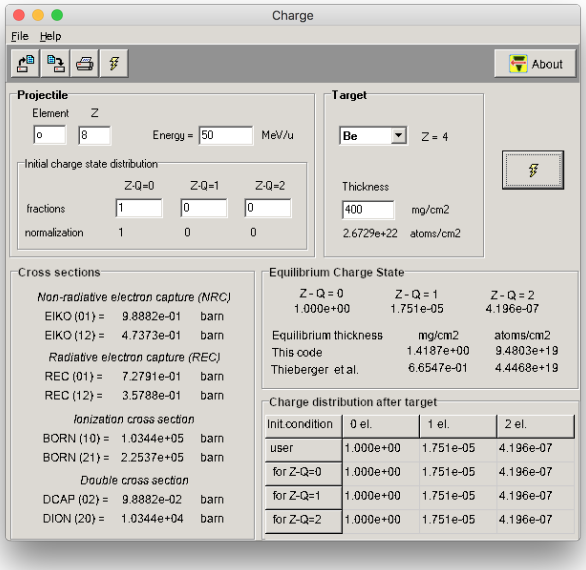

Figure 22: Charge state distribution of O ions at 50 MeV/u.

5 Memo

$^{12}C^{6+}$ beam intensity 1 nA	0.17 pnA	1.0×10^9 pps
RF frequency 76 ns^{-1}	13.158 MHz	
D3P1 dispersion 1.7 cm/%	0.59 %/cm	
D3P dispersion 4.4 cm/%	0.23 %/cm	
DA1 dispersion 0.7 cm/%	1.4 %/cm	